CPRG :0001

Coastal Processes Research Group
School of Marine Science and Engineering
University of Plymouth
Drake Circus
PLYMOUTH, PL4 8AA
United Kingdom

Contact: daniel.conley@plymouth.ac.uk

The Coastal Processes Research Group is an internationally recognised group of researchers, specialising in field studies of coastal processes. We aim to be a leading contributor to the international research community seeking to understand and predict the behaviour of coastal and estuarine systems in support of appropriate management of coastal resources and activities.

Example Research Areas

- beach morphodynamics and nearshore sediment transport
- coastal erosion and storm impacts
- video monitoring of coastal systems
- coastal process modelling
- estuarine processes and evolution

Paper details

Citation	Poate, Tim, Masselink, Gerhard, Russell, Paul, Austin, Martin, Morphodynamic variability of high-energy macrotidal beaches, Cornwall, UK, Marine Geology (2014), doi: 10.1016/j.margeo.2014.02.004		
Author(s)	Tim Poate, Gerd Masselink, Paul Russell, Martin Austin		
Corresponding Author	Tim Poate: timothy.poate@plymouth.ac.uk		
Funding bodies	SWRDA		
Paper URL publisher	http://dx.doi.org/10.1016/j.margeo.2014.02.004		
Date submitted	29-Apr-13	**Last edit date**	15-Feb-14

Marine Geology 350 (2014) 97–111

Contents lists available at ScienceDirect

Marine Geology

journal homepage: www.elsevier.com/locate/margeo

Morphodynamic variability of high-energy macrotidal beaches, Cornwall, UK

Tim Poate [a,*], Gerhard Masselink [a], Paul Russell [a], Martin Austin [b]

[a] School of Marine Science and Engineering, Plymouth University, Plymouth PL48AA, UK
[b] School of Ocean Sciences, Bangor University, Menai Bridge, Anglesey, LL59 5AB, UK

article info

Article history:
Received 29 April 2013
Received in revised form 12 February 2014
Accepted 15 February 2014
Available online 21 February 2014

Communicated by J.T. Wells

Keywords:
macrotidal
morphology
high-energy
Cornwall
beach dynamics
storm

abstract

Spatial data collected over three years are presented to assess the extent of morphological variability under seasonal and storm waves on two high-energy macrotidal beaches on the north Cornish coast. Of particular interest was the degree to which the beaches displayed bar/rip morphology and a novel approach to quantify the three-dimensionality of the beach based on the curvature of the bottom contours is adopted to identify and classify the three-dimensional beach response to changes in the dominant forcing conditions. Morphologically, the beaches range from dissipative to intermediate and are characterised by low tide bar/rip morphology which plays a key role in the nearshore dynamics and beach safety. Real-time kinematic (RTK) GPS surveys were undertaken using an all-terrain vehicle to measure the three dimensional (3D) morphology. In addition, nearshore wave data, in-situ hydrodynamic measurements, local tide gauges and Argus video data allowed detailed analysis of process–response mechanisms for long term (yearly); seasonal (monthly); storm (weekly/daily); and tidal (hourly) morphological behaviour. Both sites exhibited net long term accretion derived from the intertidal beach volume. Throughout the survey period, inter-site similarity in beach response was observed in response to storm waves, yet coupling between the seasonal wave climate and the beach morphology was not evident at either of the sites. Increased wave conditions (exceeding $H_s = 4$ m) during sustained storm events (>50 h) led to offshore transport from the beachface to the subtidal bar region. Post-storm recovery was characterised by onshore transport and the development of substantial 3D low tide morphology. Under normal wave conditions ($H_s = 1.6$ m), the dominant 3D features smoothed out as channels in-filled and bar prominence reduced over a period of 2–3 months. Overall, the beaches exhibited a significant storm-dominated morphological response cycle, unlike the more familiar winter/summer seasonal response.

1. Introduction

Most studies of nearshore morphodynamics investigating beach response to wave forcing over a range of spatial and temporal scales have focused on micro-mesotidal environments, with only few comparative macrotidal studies (Battiau-Queney et al., 2003; Masselink et al., 2007; Reichmüth and Anthony, 2007). The importance of short-term beach response to hydrodynamic conditions is clear and such studies have done much to further our understanding and modelling capabilities of coastal processes (e.g., Wright et al., 1985). Although there have been several medium to longer term (>1 year) studies into the behaviour of high-wave energy/macrotidal environments (Jago and Hardisty, 1984; Reichmüth and Anthony, 2007), as well as more intensive short-term studies (Masselink et al., 2007), these datasets have used multiple cross-shore profiles at varying alongshore spacing to assess beach response. Work by Ruggiero et al. (2005) and Hansen and Barnard (2010) has utilised longer three dimensional (3D) datasets (~5 years) to assess seasonal variability for more energetic mesotidal sites with a focus on larger scale shoreline response and beach management. There remains a relative paucity of consistent, detailed 3D morphological data from energetic macrotidal beach localities.

Rapid beach profile response to energetic wave conditions is seen most noticeably on micro-mesotidal beaches (Komar, 1985). The presence of a large tidal range forces the transitions of morphodynamic zones across the beachface, resulting not only in the suppression of morphological features (Masselink et al., 2007), but also in increased relaxation times and relatively stable beaches (Wright et al., 1982). The complex dynamics exhibited through more subtle cross-shore and longshore morphological changes on large tidal beaches requires 3D analysis over a wide spatial extent to promote understanding of such systems as a whole. Large tidal beaches at the intermediate/dissipative beach state boundary (which are always relatively high energy beaches) exhibit quasi-seasonal low tide bar/rip systems (Scott et al., 2011) which are of significant interest to beach users in terms of surfing and as potential hazards (Scott et al., 2007). The sensitivity of the 3D

* Corresponding author. Tel.: +44 1752 586181.
E-mail addresses: timothy.poate@plymouth.ac.uk (T. Poate), gerd.masselink@plymouth.ac.uk (G. Masselink), paul.russell@plymouth.ac.uk (P. Russell), martin.austin@plymouth.ac.uk (M. Austin).

http://dx.doi.org/10.1016/j.margeo.2014.02.004
0025-3227/

morphology to shifts in forcing conditions requires a multifaceted approach to further understand the dominant processes and the subsequent beach response.

This paper comprises the first long-term (3 year) dataset of monthly 3D morphological survey data collected at two high-energy macrotidal beaches. Real-time kinematic (RTK) GPS survey data are supported by almost continuous Argus images at two sites and information on the hydrodynamic forcing is provided by a nearshore directional wave buoy. The principal aim of the dataset is to assess the nature and variability of the morphological response at each site to the seasonal and storm-induced variations in the hydrodynamic forcing. Within this central aim, specific objectives are to: (1) identify the variability in 3D morphology between the two sites; (2) identify site-specific 2D/3D morphological behaviour; (3) characterise site-specific response to storm conditions; and (4) quantify the temporal and spatial variability of response under normal and storm conditions.

2. Field setting

Two study sites located on the north Cornish coast were chosen for the monitoring programme: Perranporth and Porthtowan (Fig. 1). The sites were selected to provide comparison of different beach shapes and their importance for beach users. The north Cornish coast is macrotidal (mean spring tidal range MSR 6.1 m) and exposed to a highly energetic wave climate (mean offshore $H_s = 1.6$ m) of both local wind-generated seas and North Atlantic swell (Davidson et al., 1997; Poate et al., 2009). Both beaches have a W-NW orientation and are exposed to the dominant wave approach (Table 1).

Perranporth (subsequently referred to as PPT) forms the largest survey area with a cross-shore intertidal region of 500 m and a longshore extent of 1.2 km. The wide and highly dissipative beach has a low tide beach gradient of $\tan\beta \approx 0.012$ and is composed of medium sand ($D_{50} = 0.35$ mm). The relatively high carbonate content of the sand (~50%; Merefield, 1984) suggests that offshore sediment sources are of importance. The beach is relatively featureless throughout the upper intertidal region, but a well-developed bar system interspaced with rip channels is exposed at spring low water combined with a linear to crescentic subtidal bar system (Austin et al., 2013).

To the south of PPT is Porthtowan (subsequently referred to as PTN; Fig. 2). PTN is situated in a valley flanked with high Devonian slate cliffs (70 m ODN) creating a narrow pocket beach from mid to high tide. At low tide PTN extends up to 600 m cross-shore, depending on the bar/rip morphology present, with the alongshore survey area increasing to 500 m (Fig. 2). The sediments across the lower slope ($\tan\beta \approx 0.015$) consist of medium sand ($D_{50} = 0.38$ mm; Table 1), whereas the upper beach ($\tan\beta \approx 0.05$) comprises a mixture of gravel and sand with exposed boulders during periods of sand removal resulting from beach erosion.

Wave data presented throughout this paper are derived from the directional wave buoy located off PPT which provides real-time wave data, as well as archive files for the duration of the survey schedule. Detailed summary wave conditions including significant wave height H_s, peak wave period T_p, zero-crossing wave period T_z and wave direction are presented in Fig. 3. The seasonal variability in the wave climate is evident with wave height increasing during the winter months together with long period wave conditions, whereas during the summer wave height and period are reduced. Large wave events are more prevalent during winter, although the conditions at the end of March 2010 stand out to extend this period compared with sustained calm conditions experienced for the remainder of the year. Dominant westerly waves form the majority of the wave directions and are generated during the passage of Atlantic low pressure systems; however, there is also a small, but significant, amount of energy from northerly waves which often occurs following sustained high pressures and northerly winds.

3. Method

This study uses a combination of in-situ and remote methods of data collection, complemented by data from third parties. Survey data presented here were collected using a real-time kinematic global positioning system (RTK GPS), mounted on an All-terrain Vehicle (ATV) to enable collection of morphological data over an extensive intertidal region during spring low tide. A total of 72 topographic surveys were undertaken at the two sites over a three-year period with data collection occurring during the lowest spring tide each month (~every four weeks). In addition, opportunistic post-storm surveys were also undertaken in response to energetic wave conditions.

The eastings, northings and elevation points were logged using the OSGB36 Ordnance survey grid, and were subsequently transformed with rotation and translation onto a local alongshore/cross-shore

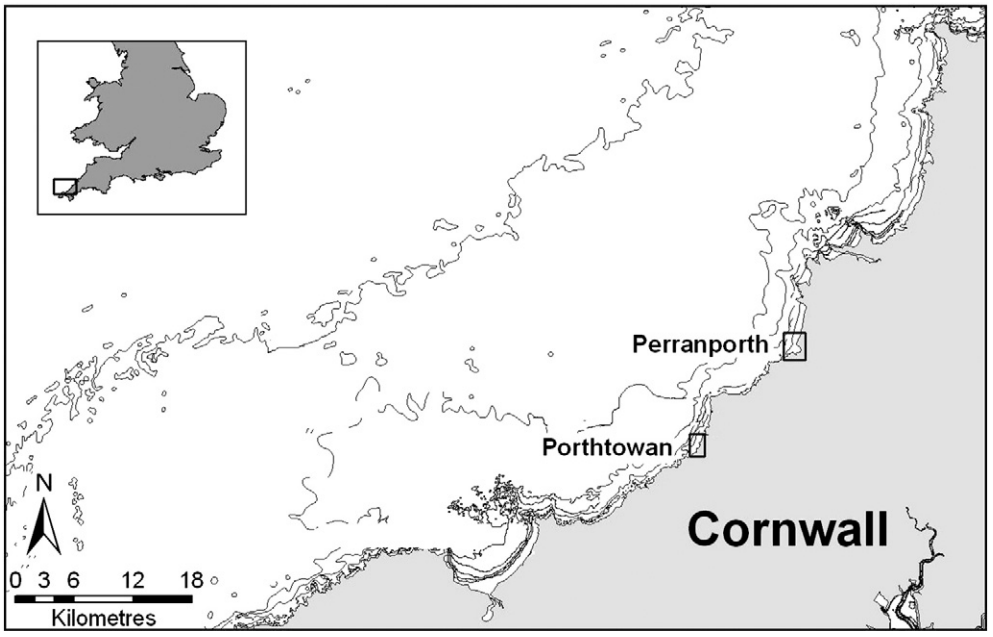

Fig. 1. Location map of the two survey sites: Porthtowan and Perranporth.

Table 1
Summary of the physical characteristic for each site.
Adapted from Buscombe and Scott (2008).

Physical characteristic				Perranporth			Porthtowan
Latitude				50°21′23.95″ N			50°17′12.92″ N
Longitude				5°9′20.92″ W			5°14′35.16″ W
Local authority				Carrick Council			Carrick Council
Management unit				Perran 7A3-09			Porthtowan 7A3-04
MSR (m)				6.15			6.0
Alongshore length (m)				1100			600–800
LW length (m)				1100			600–800
Intertidal cross-shore (m)				550			350
Average survey Area (m^2)				435000			70600
Orientation (°)				285			300
Sediment characteristics	Lower	Mid	Upper	Lower	Mid	Upper	
Intertidal gradient tan β	0.012	N/A	0.038	0.015	N/A	0.045	
Sediment classification	Sand	Sand	Sand	Sand	Sand	Gravel and sand	
Mean (Φ, mm)	−2.21 (0.22 mm)	−1.98 (0.25 mm)	−1.71 (0.31 mm)	−2.33 (0.20 mm)	−2.34 (0.20 mm)	−2.46 (0.18 mm)	
Mean fall velocity w_s ($m\ s^{-1}$)	0.046	0.040	0.033	0.050	0.053	0.055	
$CaCO_3$ %	43.80 ± 8.80	N/A	N/A	55.70 ± 6.48	N/A	N/A	

coordinate system which was identical to the grid used by the Argus video data (see below) to aid interpretation and comparison. The generation of a 3D digital elevation map (DEM) was the basis for subsequent interpretation and analysis and a reliable quadratic loess interpolation approach was adopted with raw data interpolated onto a regular 1-m grid (Schlax and Chelton, 1992; Plant and Holland, 2008). Calculation of the intertidal beach volume was undertaken for each site and each survey from the interpolated surface. Net change (Δz_{net}) and the absolute change (Δz_{max}) were generated from the interpolated surface plots with the vertical change (m) presented for each 1 m^2 grid cell. Because of the highly dynamic nature of the low tide region, which restricted survey coverage and therefore subsequent comparison with previous surveys, a reduced region was defined. For each site, the intertidal volume was split into 3 regions to differentiate between the upper, mid and lower beach. The definition of these regions was based on the relative tidal position for each site; upper beach (MHWN–upper survey extent), mid beach (MHWN–MLWN) and lower beach (MLWS–MLWN). Cross-shore transects were extracted for 2D analysis of each survey, from which, the net change (sum of all surveys) and the profile envelope (min and max of the profile) were calculated.

In addition to in-situ measurements of beach morphology, remotely sensed images are collected at PTN and PPT. An existing site at PPT (two cameras), which was first established in 1993 (Davidson et al., 1997), was re-established following replacement cameras in 2006. At PTN a new Argus installation consisting of 4 cameras covering the full intertidal beach and offshore bar/rip system was installed in September 2008.

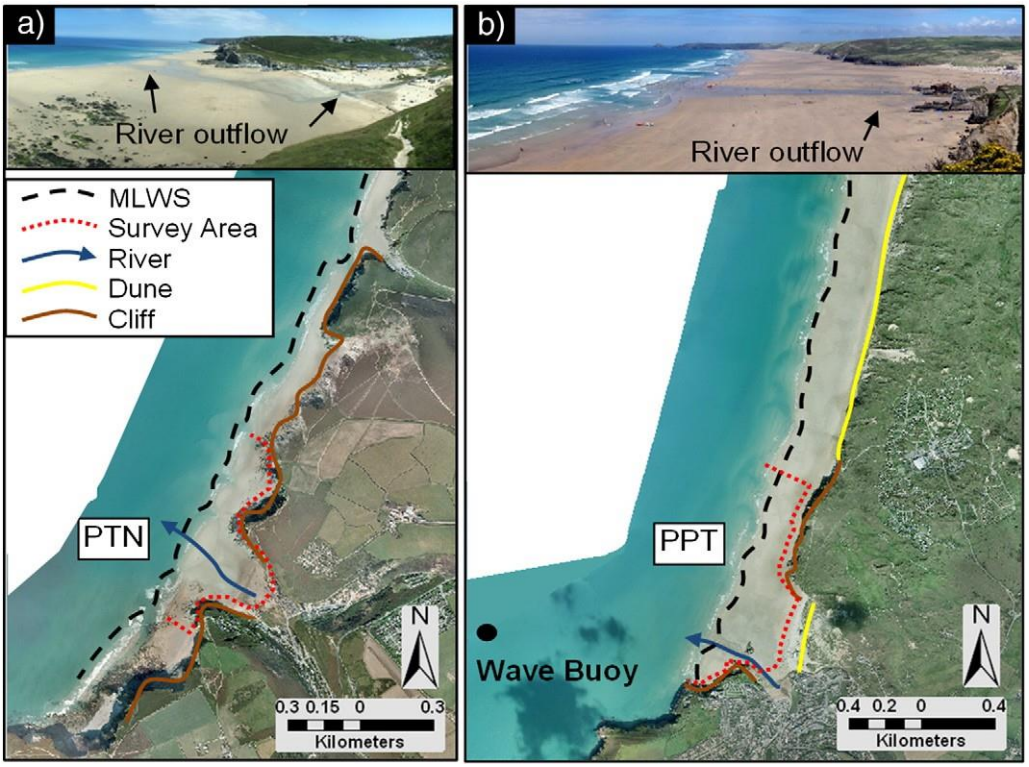

Fig. 2. Panoramic photographs of Porthtowan (PTN) looking north (a) and Perranporth (PPT) (b). The aerial photograph shows both PTN and PPT. The black dashed line in the aerial photograph represents the position of MLWS, the red dashed line demarcates the survey areas and the blue arrow highlights the river output across the beachface. (For interpretation of the references to colours in this figure legend, the reader is referred to the web version of this article.)

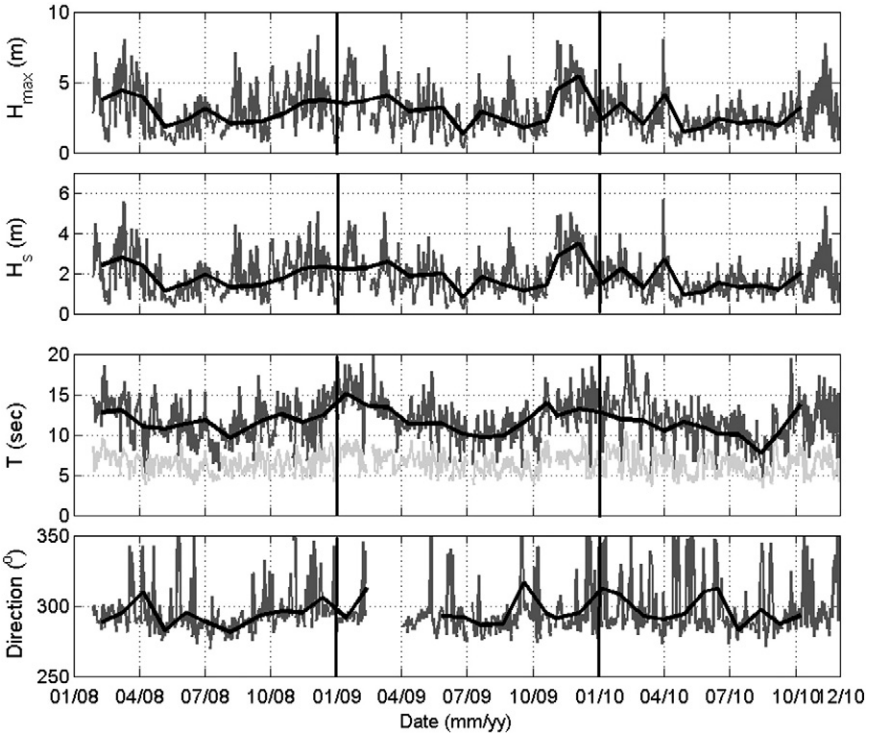

Fig. 3. Summary wave statistics from the nearshore wave buoy at PPT (depth 10 m CD) for 2008–2010. From top to bottom: maximum wave height H_{max}, significant wave height H_s, peak wave period T_p, zero-crossing wave period T_z (light grey) and wave direction. Black lines show monthly average, vertical black lines delineate year boundaries. Gaps in the wave direction record are due to buoy faults.

Both sites provide half-hourly digital "image products" consisting of a single snapshot image, a time-exposure image and a variance image (Holman and Stanley, 2007). For both sites, conversion from image coordinates (u, v), to real world co-ordinates (x, y) was undertaken using well established methods for Argus video systems (Holland et al., 1997). The detection of subtidal bar positions was one of the first outputs identified from Argus images (Lippmann and Holman, 1990). Van Enckevort and Ruessink (2001) further developed this idea with a detection algorithm which finds the maximum intensity value for cross-shore pixels and which has specific relevance to regions of high intensity where wave breaking occurs. The BarLine Intensity Mapper (BLIM) tool provides a useful method to utilise this algorithm for the detection of bars from rectified Argus images. Previous work has shown that the positional accuracy of this approach is affected by breaker height and water level (Kingston et al., 2000; van Enckevort and Ruessink, 2001), and, owing to the energetic conditions and the macrotidal range, the number of suitable images for BLIM analysis was constrained before image quality was considered. For the purpose of this work the following criteria were applied to select suitable images: (1) water level between −3.5 m and −2.5 m Ordnance Datum Newlyn (ODN) for PPT, and −2.8 m and −1.5 m (ODN) for PTN; and (2) wave height $H_s \geq 0.5$ m and $H_s < 1.5$ m to provide the greatest chance of wave breaking on the bar, without causing an excessive increased breaking zone which would reduce positional accuracy. In the absence of nearshore surveys, to validate the BLIM bar detection accuracy, the bar position was primarily used for qualitative bar behaviour analysis.

The BLIM tool allows determining the cross-shore bar crest position which can be used to determine long-term migratory patterns of bars to be linked with wave conditions. In addition, the rectified images also yield information on the bar shape and have been used to provide subtidal morphological classification of the sites (see Section 3.2).

Beaches which lie on the boundary between dissipative and intermediate classification experience a range of morphological features from highly planar to low tide bar/rip systems. Within these broad classification states, the morphology can be grouped further to identify dominant features and modal morphology. A key part of this paper concerns being able to quantify the variability observed at a beach at any given time, and relate this to wave forcing and the antecedent morphology. Building on an approach adopted by Smit et al. (2008), who looked at shoreline variability from Argus waterlines to identify beach resetting following storms, a measure is used by which a relative level of 3D is assigned to each survey. Although the term "3D" suggests that a volumetric component is incorporated, in the present approach the primary objective is to quantify the surface shape and intuitively the term 3D is adopted in keeping with current terminology. In order to quantify the degree of 3D in each survey, contour lines were extracted between 0.2 m ODN (mean sea level) and −2.4 m ODN (0.2 m above low water springs) at 0.2-m intervals from the monthly topographic data. A "curl value" (CV) was then computed using the ratio of total contour length and the straight line length of the contour, where CV = 1 represents a planar featureless intertidal region and CV ≥ 1.5 indicates a highly variable shoreline (Fig. 4). For each survey the CV was computed for contours between 0.2 and −2.4 m ODN from which the mean value of the highest third ($\overline{CV}$) was recorded (Fig. 4). To ensure that the automatic routines were a realistic representation of the conditions presented in a surface elevation map, the opinions of relevant researchers within this field were sought to verify the results. Following the same approach as Ranasinghe et al. (2004), 10 "experts" were asked to rank the same monthly surveys for levels of 3D on a scale of 0–100 providing a comparison of the accuracy of the automatic 3D classification methods. Comparison between the automatically-derived $\overline{CV}$ values with the expert assessment yielded a p-value of < 0.002. The relative shifts in the 3D parameters each month are crucial for identifying trends in morphological response between the sites and to the forcing conditions. Importantly 80% of the changes in 3D level as indicated by changes in $\overline{CV}$ values was also recognised by the experts.

Section 4.2 details specific storm responses at the field sites. Individual storm events were classified using the peaks-over-threshold approach, with storms classified as having an $H_s \geq 4$ m and a duration ≥ 1.5 h.

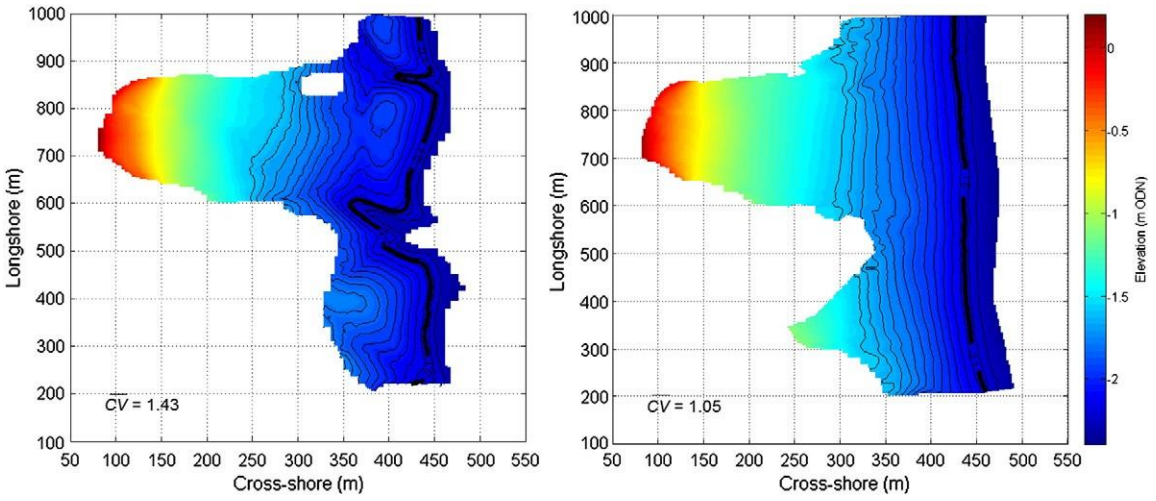

Fig. 4. Digital elevation models for PTN showing contours used for 3D analysis. Left panel shows a highly 3D surface from May 2009; right panel shows a relatively featureless beach from October 2010. The difference in prominence of the 3D morphology is quantified using the $\overline{CV}$ values.

4. Results

4.1. Net intertidal morphological change and morphological variability

PTN exhibited the greatest range of morphological response across the full cross-shore extent of the beach. The beach is dominated by an episodic low tide bar/rip system characterised by persistent seaward-directed channels located at the cliff base (cf., Fig. 4). Morphological response is evident across the length of the profile at PTN however two peaks are evident with the first present below MLWN and the second identifying the significant response observed at the top of the profile through the intermittent development of a high tide berm (Fig. 5). Unlike PTN there was no significant development of a berm at PPT throughout the surveys, but, instead, the growth of low tide bar/rip systems dominated throughout.

The long term 3D variability of surface change at PTN and PPT is presented in Fig. 6. Due to the dynamic nature of the shoreline the survey coverage does not provide complete comparison for the furthermost seaward limit; however, clear regions of maximum net Δz are visible for the lower beach. This observation is further expressed through the absolute change in surface elevation, calculated as the sum of the monthly Δz, which highlights the region between MLWN and MLWS, cross-shore 400–500 and 450–600 for PTN and PPT respectively, as the most dynamic. Importantly, the absolute surface change also highlights the variability at the top of the beach for PTN, which is a result of the episodic berm development along the MHWS line referred to previously (Fig. 6).

Four different beach states were identified (Table 2): "planar", "low tide rhythmic", "low tide rhythmic/channel" and "low tide bar/rip" using the 3D topographic surface plots such as those presented in Figs. 4 and 8 and are based on Scott et al. (2011). These states build on the present literature and will be further incorporated into the subtidal variability discussed in Section 4.2. This classification highlights the lack of a significantly more prevalent state occurring at either site; however planar conditions occur least frequently. For clarity throughout this paper a transition from planar to low tide bar/rip is referred to as increasingly 3D, whereas the development of decreased 3D morphology is referred to as a 2D shift.

The morphological evolution for both sites, including the net volume, the qualitative beach state and the $\overline{CV}$, is presented alongside the wave conditions during the survey period (Fig. 7). Both sites experienced net accretion over the survey period which was punctuated by four significant drops in net volume highlighted by the arrows in Fig. 7. The shift in net volume helps to further explore the long term behaviour in the beach state classification and the 3D $\overline{CV}$ values which highlight distinct increased 3D morphology following sediment removal in February 2009 and November 2009 for both sites. Both the qualitative descriptions of beach states and the quantitative $\overline{CV}$ values

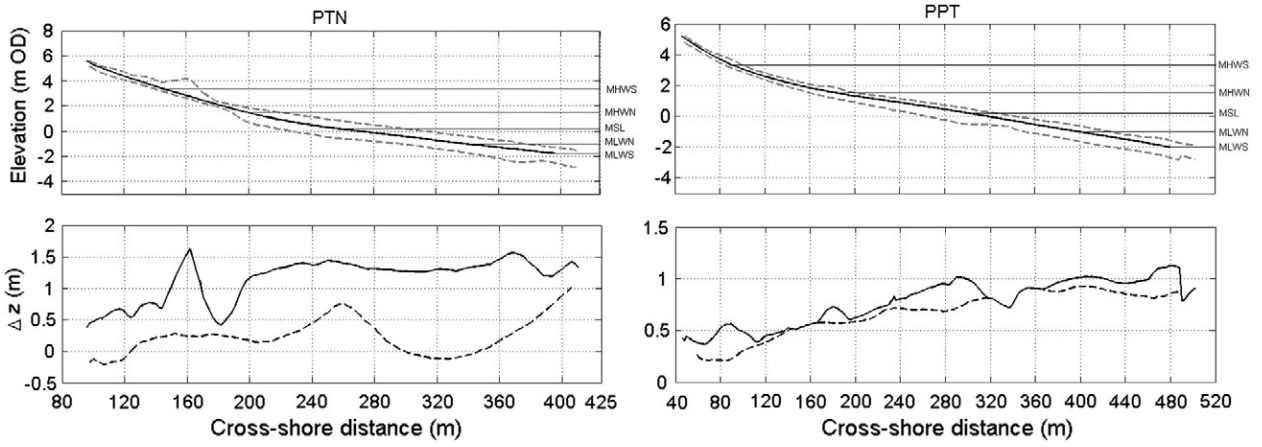

Fig. 5. 2D profile variability for PTN (left) and PPT (right): top panel shows mean profile shape (solid line) with profile envelope (dashed lines); bottom panel shows the net profile change (Δz_{net} dashed line) and profile envelope range (Δz_{max}, solid line); for position of the profile line refer to Fig. 6.

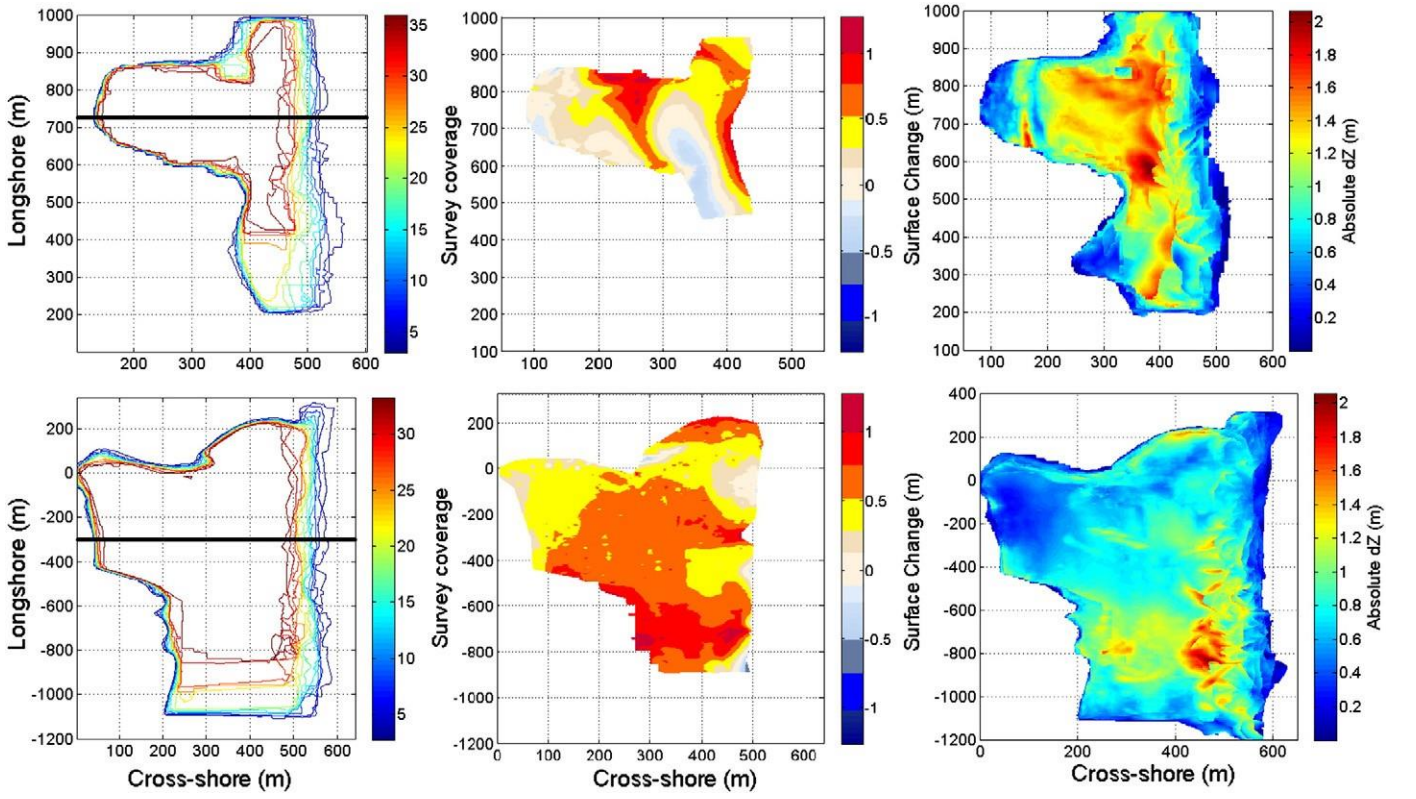

Fig. 6. 3D variability at PTN (top) and PPT (bottom); left plot shows contour map showing survey perimeter to aid interpretation; net change over survey period (Δz_{net}, middle panel); absolute change (Δz_{max}, right panel). The horizontal black line shows the location of the 2D profile extracted in Fig. 5. Surface change in m represents vertical change for each 1 m^2 grid cell.

show good agreement, in the 2D and 3D shifts, supporting the inclusion of this approach in further assessments of morphological response. Despite the seasonal pattern in the nearshore wave climate, the morphological behaviour exhibits poor seasonal trends.

A pattern in the net volume loss, in response to energetic waves, and the initial rapid rise in $\overline{CV}$ as the beach recovers highlights a dominance of storm events over the seasonal wave climate on the morphology response. The complexities of the storm response are addressed further in Section 4.3, however the process of 2D evolution, observed during the longer term (months) recovery phase following storm events, is well represented in Fig. 8 which highlights the infilling and smoothing of the lower beachface.

4.2. Subtidal bar dynamics

Similar to the intertidal responses observed at PTN and PPT, the Argus images indicate a range of variability within the subtidal states of the nearshore region which were manually categorised (Fig. 9). To maintain consistency and aid comparison, the key "states" have been grouped under headings dominant in recent literature and include the generally accepted sequence of stages associated with transition from 2D dissipative planar beaches with a longshore bar–trough system to 3D through crescentic bars, attached crescentic bars and transverse bars intersected by dominant rip channels. A multi-bar state has also been recognised.

Table 2
Percentage occurrence of beach states for individual sites.

Site	Percentage occurrence of beach state			
	Low tide bar/rip	Low tide rhythmic/channel	Low tide rhythmic	Planar
PTN	30	19	32	19
PPT	30	30	30	10

There is little evidence of a seasonal cycle in bar behaviour or dynamics at PTN. At the start of the image collection (September 2008) the system was dominated by low tide bar/rip morphology, affecting the breaker pattern at the shoreline, with little evidence of a subtidal shore parallel bar. Throughout the 2008/2009 winter the subtidal region developed with complex transverse bars defining the breaking zone. Intensive storm events during Nov–Dec 2008 (discussed further under Section 4.3 Storm response) resulted in the formation of an alongshore rhythmic bar. Following continued storms in January, further material was moved offshore from the intertidal region and in-filled sections of the subtidal trough between the shoreline and the existing bar (Fig. 9). The resulting highly crescentic attached system remained dominant at PTN throughout most of 2009, while the intertidal beach volume gradually increased.

Energetic storm conditions during Nov–Dec 2009 (discussed further below) caused widespread redistribution of intertidal sediment to the subtidal region, resulting in detachment of the bar to the north and a build-up of material in the centre of the survey area, forming a complex multi-bar system. Over the subsequent 3 months this material gradually moved onshore, resulting in the creation of an extensive low tide bar system. Under continued onshore movement this bar gradually merged fully with the shoreline resulting in a small single bar that was still present in the nearshore region by April 2010 (Fig. 9).

During the remainder of 2010, the bar continued to move onshore and weld with the shoreline, which became increasingly 3D as low tide channels developed. However, these were small-scale features and not sufficiently developed to withstand destruction during energetic wave conditions in September/October 2010 which left the intertidal beach relatively featureless. Following intensive storm events in November, resulting in a loss of material from the intertidal region, a longshore bar/trough developed.

At the start of 2008, PPT exhibited a complex system with a subtidal longshore rhythmic bar and well developed low tide bar/rip morphology.

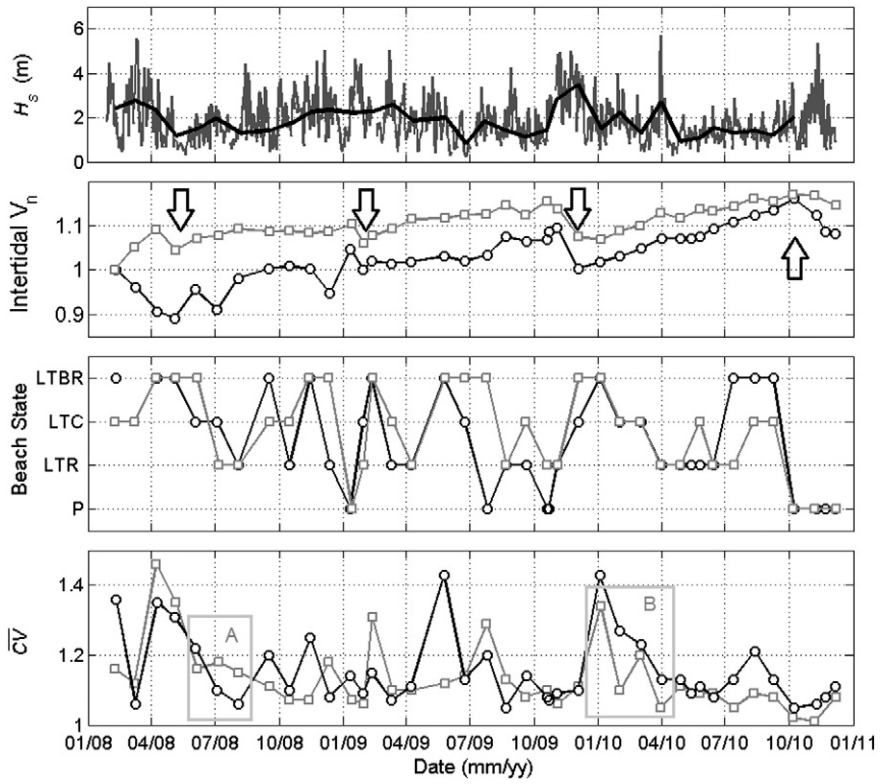

Fig. 7. Summary plots of significant wave height H_s with monthly average H_s (black) and morphological response for PTN (black) and PPT (grey); normalised intertidal volume V_n (second panel); assigned qualitative beach state (third panel); contour derived $\overline{CV}$ (fourth panel). Box A and B identify the 2D transition presented in Fig. 8 for PTN and PPT respectively.

This developed into a more pronounced transverse bar system as these channels extended offshore through the breaker line during the calmer summer wave conditions. As conditions became increasingly energetic (Nov/Dec) the low tide rips intersecting the longshore bar were removed and the system was defined by a crescentic longshore bar which remained attached at the centre of the survey area. Throughout 2009 and much of 2010 this state dominated with the position of the alongshore attachment of the bar the only change observed (Fig. 9).

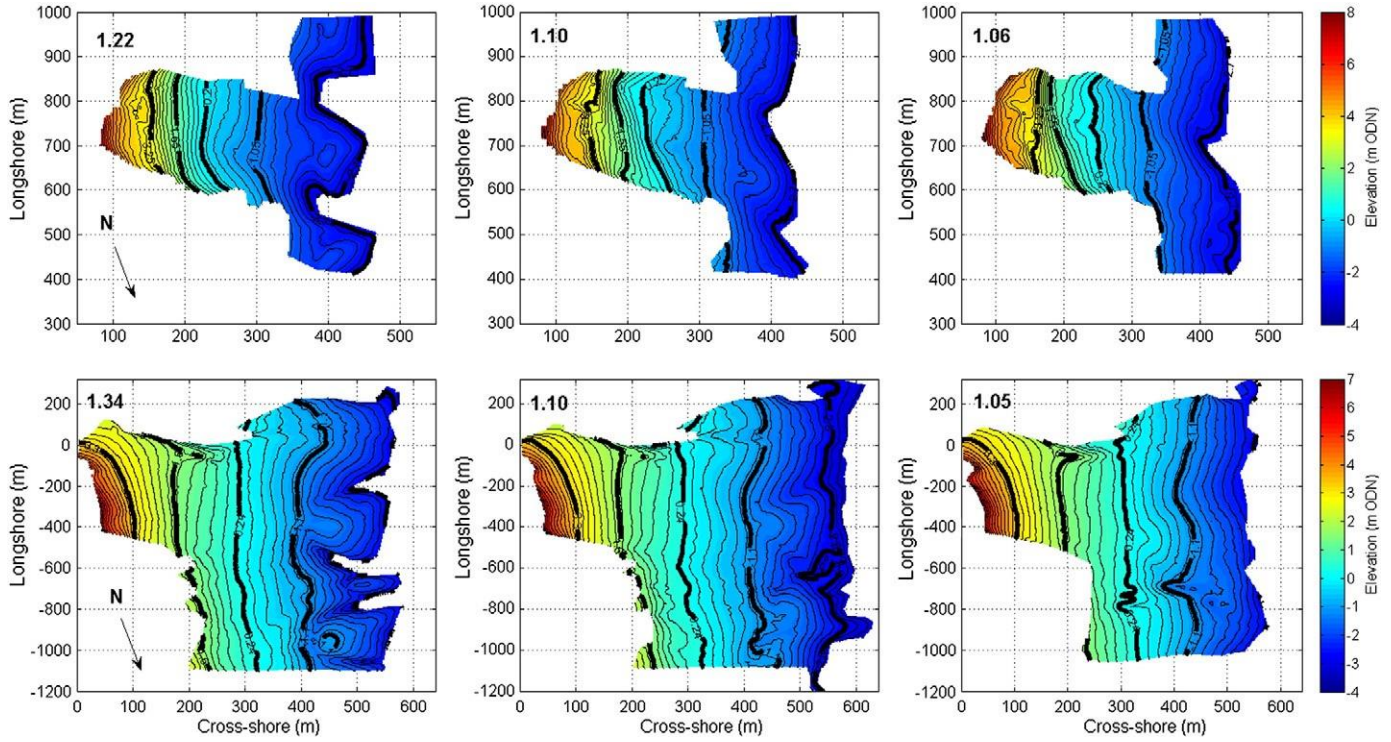

Fig. 8. Sequential 2D morphological evolution. The top panel shows monthly surface plots for PTN from June, July, and August 2008, and the bottom shows PPT from January, February, and April 2010. $\overline{CV}$ values for each survey are overlaid; thick black contours identify MLWS, MLWN, MSL, MHWN and MHWS.

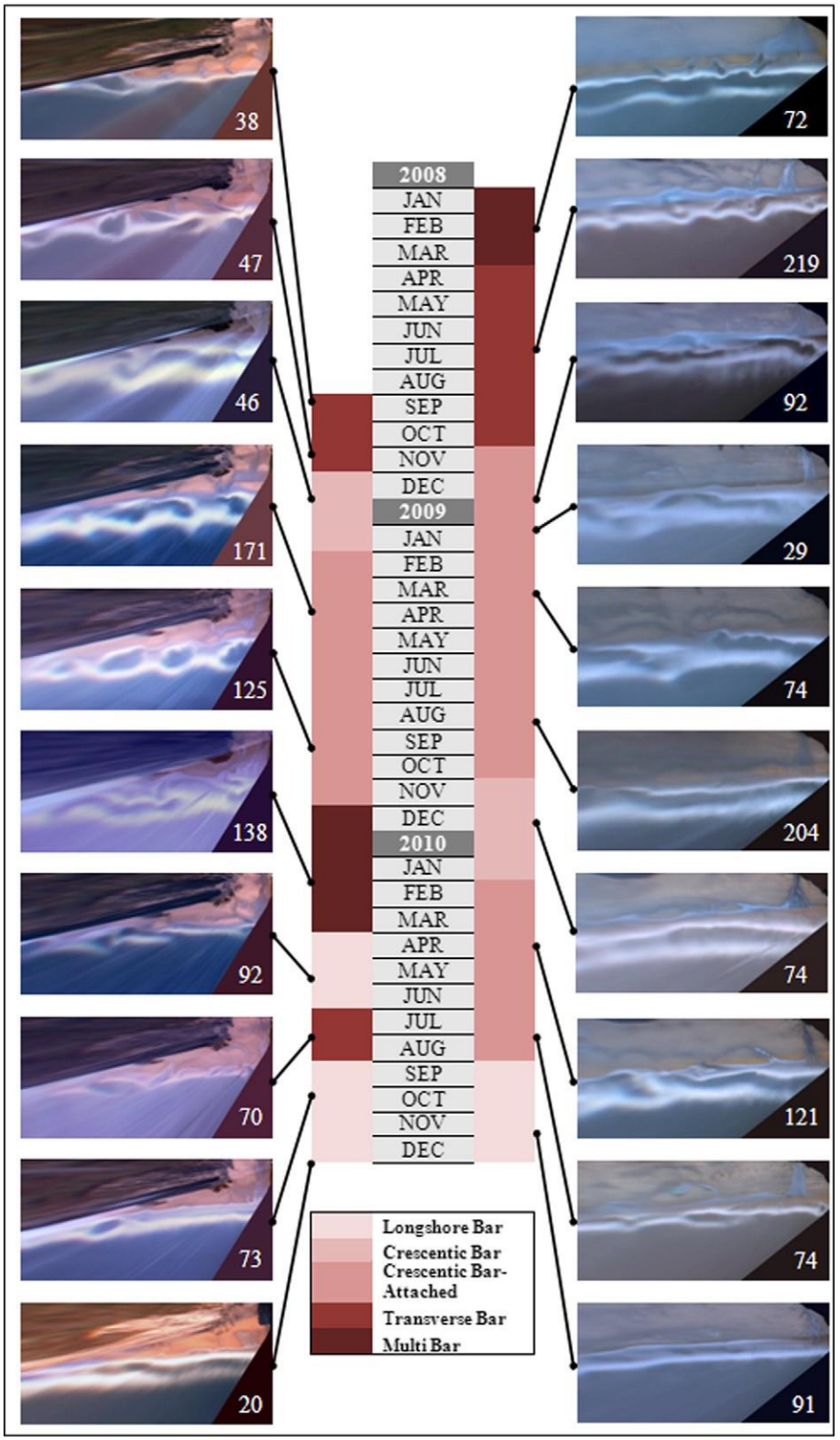

Fig. 9. Subtidal classification (red shading) for PTN (left column) and PPT (right column) throughout the 3-year survey period. Images depict breaker patterns present during relevant phases while the numbers correspond to the approximate number of days that the depicted bar shape lasted. Bars are classified as Longshore Bar, Crescentic Bar, Crescentic Bar Attached, Transverse Bar and Multi Bar, based on similar classifications by Short (1996).

Storm conditions in November 2009 resulted in the bar detaching and a crescentic longshore state developed; however, by February 2010 a transverse connection with the shoreline became re-established (Fig. 9). Calm conditions throughout most of 2010 led to the bar reducing in size and moving closer to the shoreline. More energetic conditions from September onwards resulted in a similar response to that observed at PTN with a longshore shore parallel bar developing, although again full detachment from the shoreline did not occur.

The rectified Argus images provide some indication of in-phase coupling, particularly during September and October 2009, of the crescentic

longshore bar and the shoreline at PTN (Fig. 9), however, the relatively short length of the dataset and the variability in the subtidal bar shape restrict a more detailed analysis. While PTN and PPT are characterised by a single bar (evident from the Argus images), the low tide bar development has been shown to be well correlated with the bar behaviour following storm events, continued image collection at both sites will enable further work on this trend to be undertaken.

4.3. Storm response

Nearshore wave data from PPT was used to identify periods of energetic conditions throughout the survey period. Storm distribution follows a strong seasonal behaviour with peak events occurring during winter months (Fig. 10). While individual storms exhibited similar values of significant wave height and wave period, the cumulative duration of events between surveys identifies specific periods during which sustained storm-dominated wave conditions were experienced (Table 3).

Using duration of storm events as a measure of erosive conditions we see strong correlation with periods of widespread sediment loss in February 2009 and December 2009 in response to N90 h of energetic wave conditions; conversely, there is poor correlation with the sediment removal observed at PPT and PTN in November 2010 with b 20 h of storm conditions. In addition there is disparity in the response to N60 h of storms in March 2008 with PTN experiencing loss while PPT experienced a net increase in beach volume (Table 3). From the 27 individual storm events detailed in Table 3, storm analysis has been undertaken for 12 storm periods using pre- and post-survey data as close to the storm events as available (Table 3). As identified in the Morphology (Section 4.1), the maximum morphological response at all sites generally occurs between MLWN and MLWS, but for macrotidal regions the ability to obtain comparative data severely restricts the ability to survey immediately prior to or immediately following a storm. In addition, the nature of highly dissipative beaches means that cross-shore run-up distances can be in the order of 200 m, again restricting access to the region of interest. Because of this, the pre/post- storm intervals are often larger than ideal, and as such the Argus images are used when possible to aid interpretation. Summary intertidal response, incorporating beach state and volume, from PTN and PPT, is presented in Table 3. This highlights the similar response observed between both sites from 2009 to 2010, where we see 3D shifts in intertidal morphology in conjunction with drops in beach volume following sustained periods of energetic conditions.

Table 3
Summary of storm activity between surveys and the beach response observed for PTN and PPT. Periods in bold/dashed boxes highlight matching response at each site.

Storm period	Duration of storms. (h)	Storm impact (No/h)	RTR	Beach response (up–state/down–state)		Volume (increase = + decrease = –)	
				PTN	PPT	PTN	PPT
Mar–Apr 2008	**63.5**	**13**	**0.84**	**Down**	**Down**	–	+
Aug–Sept 2008	15.5	8	1.09	Down	Up	+	–
Nov–Dec 2008	39	19	0.81	Up	Down	–	+
Jan 11th–Jan 29th 2009	**94.5**	**47**	**1.07**	**Down**	**Down**	–	–
Feb–Mar 2009	19	19	1.09	Down	Up	–	+
Aug–Sept 2009	7	7	0.79	Up	*NC*	–	–
Nov–Dec 2009	**109**	**18**	**1.19**	**Down**	**Down**	–	–
Dec 2009–Jan 2010	**2**	**2**	**1.56**	**Down**	**Down**	+	–
Jan–Feb 2010	**2.5**	**2.5**	**0.88**	**Up**	**Up**	+	+
Mar–Apr 2010	**19**	**19**	**1.48**	**Up**	**Up**	+	+
Oct–Nov 2010	4	4	0.38	*NC*	*NC*	–	–
Nov–Dec 2010	46.5	47	0.74	*NC*	*NC*	–	–

NC = no change.

However, where storm events are more short lived the transitions are predominantly mixed, reflecting no coherence between sites.

4.3.1. Storm event November 4th 2009–January 31st 2010

November 2009 to January 2010 was a period characterised first by significant storm activity which led to the widespread removal of material at both PPT and PTN (Fig. 7), followed by a period of calm. Between the surveys in November and December there were 6 separate storm events resulting in the 5% exceedance H_s reaching 4.7 m, 50% exceedance H_s = 2.8 m and the 90% exceedance H_s = 1.46 m, representing the largest exceedance waves throughout the 3-year survey period (Figs. 3, 11). Following the November storms December experienced a very calm wave climate with 50% and 90% exceedance H_s = 1.2 m and 0.69 m respectively.

Widespread removal of material occurred at both sites across the majority of the beachface from MHWN down (Fig. 12) with the greatest

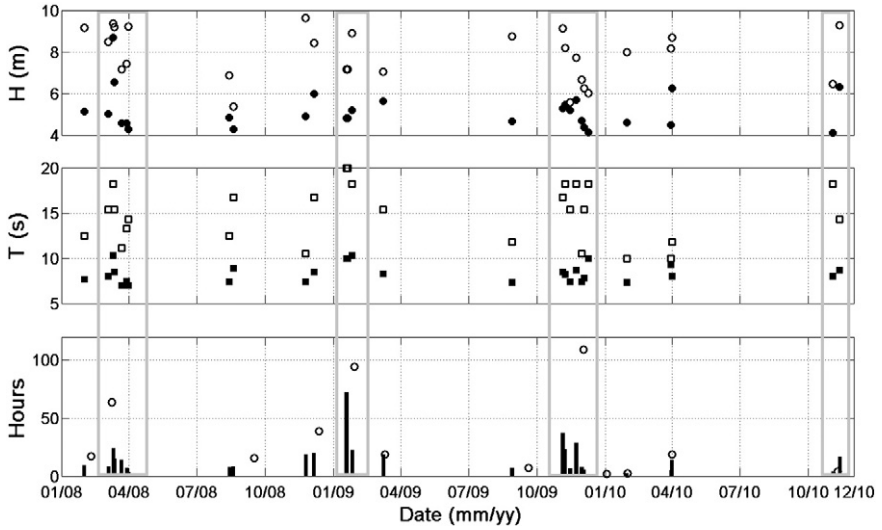

Fig. 10. Summary storm statistics derived from data presented in Table 3. From the top; peak significant wave height (H_s black circles, H_{max} hollow circles), peak wave period (T_z black squares, T_p hollow squares) and duration of individual storm events (bars) with the total storm durations between individual surveys (hollow circles, h). Grey boxes indicate periods of intertidal loss observed at most sites (cf., Fig. 7).

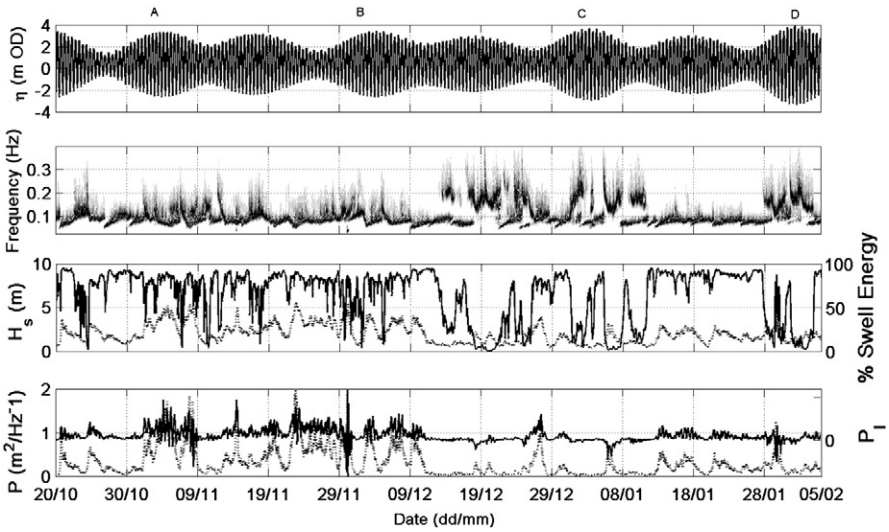

Fig. 11. Summary of the wave conditions present between November 2009 and February 2010; from top to bottom: still water level η; wave spectrum; significant wave height H_s (dashed line) and % swell energy (solid line); wave energy flux P (dashed line) and longshore component of the offshore wave energy flux P_l (dashed line), where positive indicates northerly directed. The letters A–D identify times of beach surveys.

loss in the lower to mid region. Although both sites experienced extensive removal under the sustained storm conditions, the surface morphology remained fairly rhythmic at the shoreline, with a bar feature evident at PPT. By January the calm conditions lead to onshore accumulation at both beaches and a 3D transition; at PTN the upper and mid beachface increased in volume and two large low tide bars formed at the shoreline, while PPT also developed highly 3D bar/rip morphology (Fig. 12). Wave conditions remained relatively calm throughout January with 50% exceedance H_s = 1.58 m. By February the beaches remained 3D; however, in-filling of the channels resulted in a smoother and less 3D low tide region as reflected in the $\overline{CV}$ values (Fig. 12).

At both sites the Argus images highlight the shift in nearshore bathymetry in response to the storm conditions; at PPT the shoreline moves landward while a secondary breaker line develops between the shoreline and the subtidal bar indicating a build-up of material causing

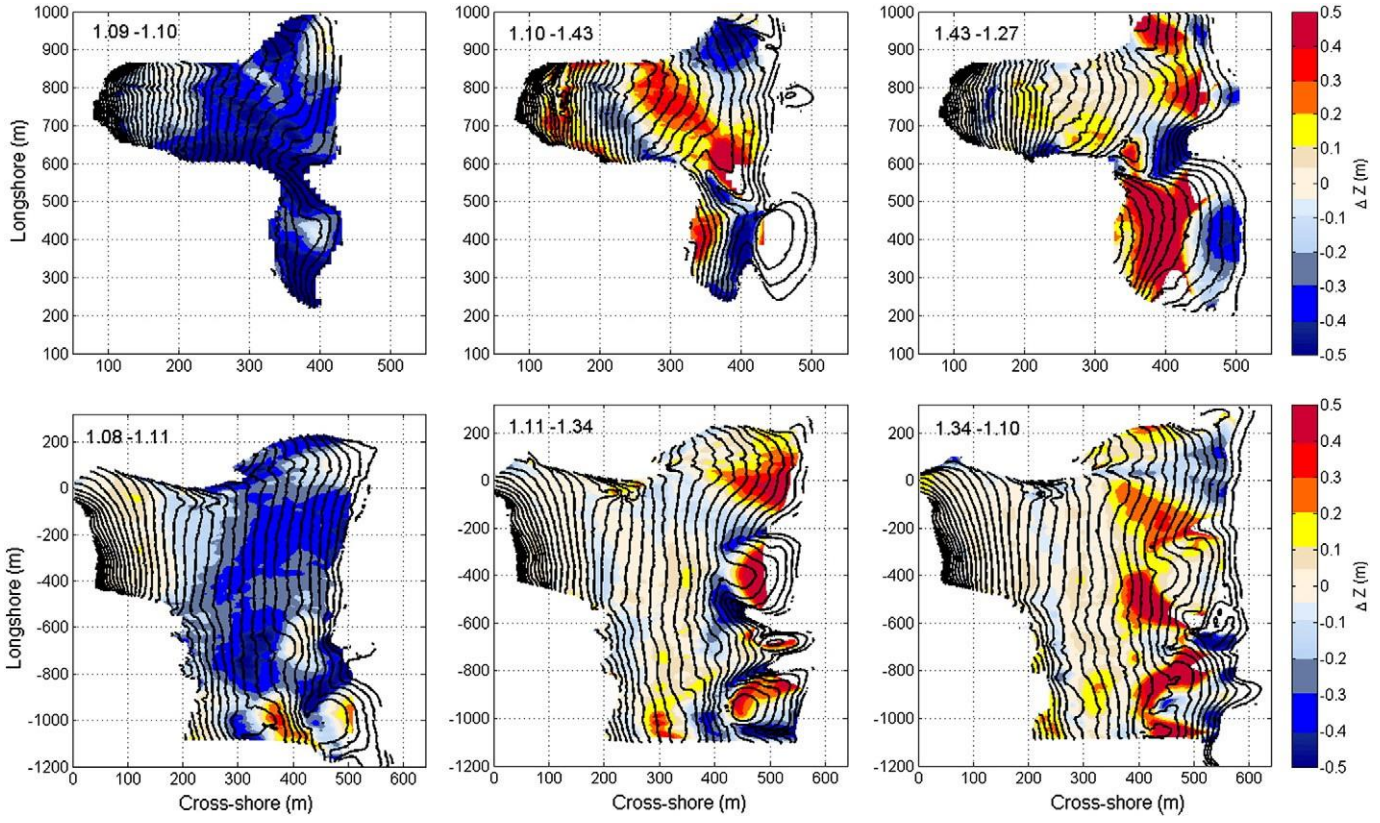

Fig. 12. Surface plots showing Δz for November–December 2009, December–January 2010 and January–February 2010 for PTN (top row) and PPT (bottom row). Colours indicate regions of accretion (yellow/red) and erosion (blue). Contour lines show the subsequent morphology. $\overline{CV}$ values are provided in the top left of the plots.1. (For interpretation of the references to colours in this figure legend, the reader is referred to the web version of this article.)

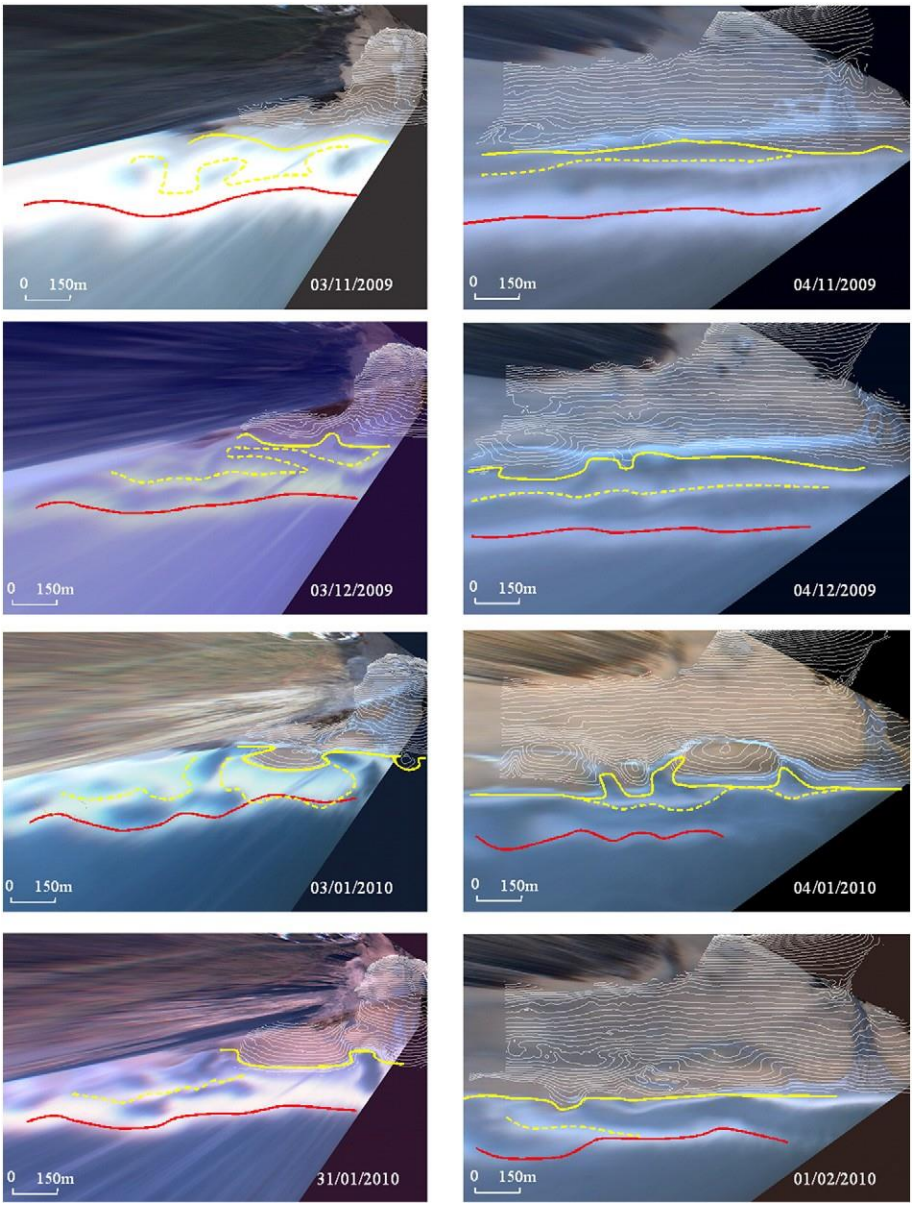

Fig. 13. Plan-view rectified Timex images from PTN (left) and PPT (right) with contours of intertidal morphology overlaid. Images show transition between November 2009 (top row) to January 2010 (bottom row). Offshore bar position (red line), shoreline breaker position and nearshore breaker zone (solid and dashed yellow line). Note the November Argus images are taken during large wave conditions and so positions are approximate. (For interpretation of the references to colour in this figure legend, the reader is referred to the web version of this article.)

secondary breaking in this region. At PTN the rhythmic shoreline and nearshore breaker pattern which was stable for the preceding 125 days (Fig. 13) is redistributed with more complex longshore/cross-shore channels present.

Overall following sustained storm events throughout November ($H_s \geq 4$ m for 109 h) widespread removal of material was observed at both sites. Over the following two months reduced wave conditions with no storm events resulted in onshore transport from the subtidal area to the low tide beachface, resulting in the formation of large well developed 3D shorelines. Under more mixed wave conditions these channels became in-filled and the 3D features were gradually smoothed.

4.3.2. Storm event January 4th 2009–March 13th 2009

The start of 2009 was characterised by a period of sustained energetic waves (N90 h) during mid-January with wave heights peaking at $H_s = 5$ m (Fig. 14). This was followed by a period of calm through February before a short event with wave heights in excess of $H_s = 4$ m prior to the March survey. As with the storm in November, widespread erosion occurred at both PTN and PPT, particularly over the lower beachface which led to decreased $\overline{CV}$ values through smoothing of the morphology (Fig. 15).

The post-storm recovery phase was characterised by onshore accretion and increased 3D morphology across the lower beach (Fig. 15). Accretion continued in response to the calm conditions of February; however, the 3D morphology was reduced as channels in-filled and bars merged. It is also likely that the short energetic event prior to the March survey resulted in some smoothing of the beachface (Fig. 15). The occurrence of storm conditions coinciding with the neap phase of the tidal cycle may have additional impacts on the response however no clear connection is apparent, highlighted in Table 3 using the RTR. Equally the role of swell/wind waves is also likely to be of importance in determining the response yet the timescales involved make such connections more complex.

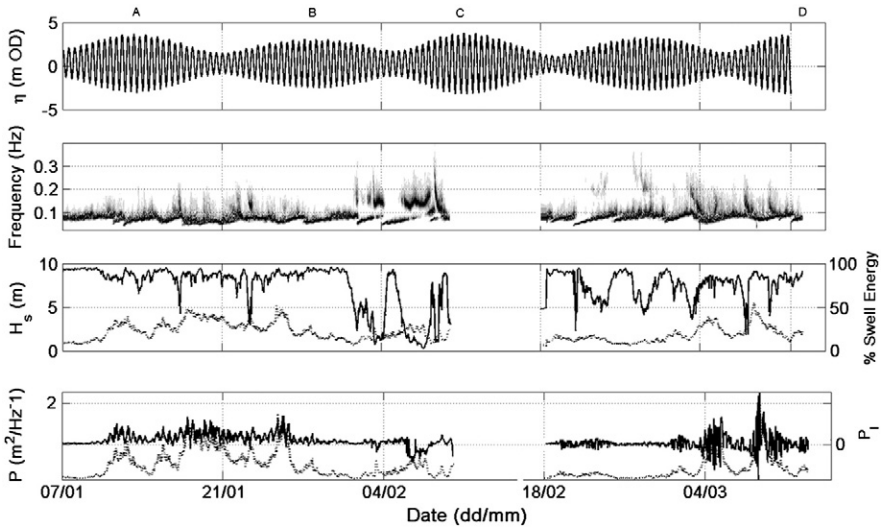

Fig. 14. Summary of the wave conditions present between January 2009 and February 2009; From top to bottom: still water level η; wave spectrum; significant wave height H_s (dashed line) and % swell energy (solid line); wave energy flux P (solid line) and longshore component of the offshore wave energy flux P_l (dashed line), where positive indicates northerly directed. The letters A–D indicate beach surveys.

5. Discussion

On a coast-wide scale, the long-term behaviour has been very similar between PTN and PPT with both exhibiting almost identical growth and decay in net beach volume. Although there are periods of net volume loss, at both sites there has been a progressive increase in beach volume, which reflects the decrease in storm events and storm durations throughout the survey period (Poate, 2012). With only three years of relevant data, and conflicting accounts from long term local residents with regard to previous sand levels, a clear interpretation is complex.

To characterise the complexity of the system and build on previous efforts to describe shoreline variability by Smit et al. (2008), the $\overline{CV}$ allows long term datasets to be quickly analysed and periods of transition to be identified. The results presented here show significant variability in beach morphology at PPT and PTN, with bar/rip systems dominating the low tide region. While there is fairly good agreement in the development and removal of such features between the two sites, of interest is

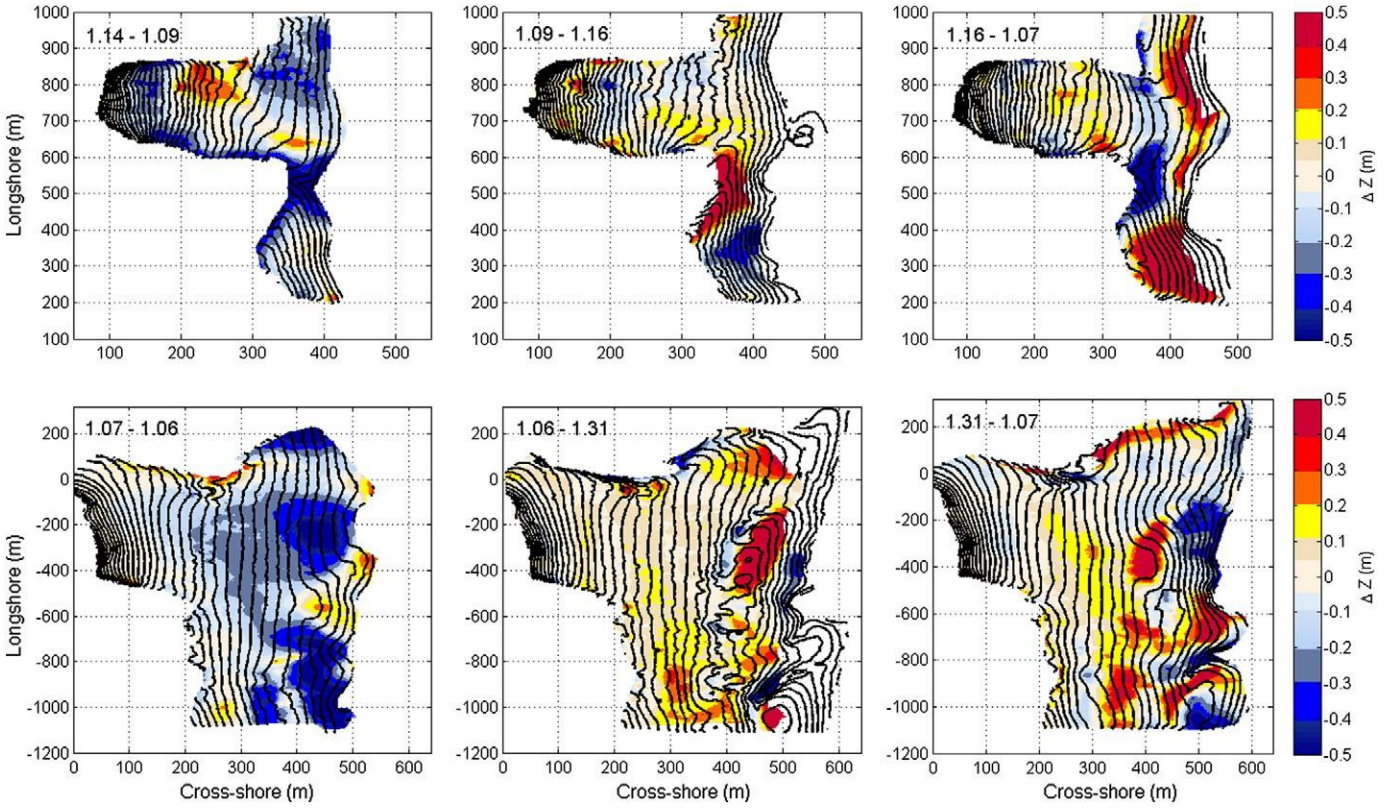

Fig. 15. Surface plots showing Δz for January (13th)–January (30th) 2009, January (30th)–February 2009 and February–March 2009 for PTN (top row) and PPT (bottom row). Colours indicate regions of accretion (yellow/red) and erosion (blue). Contour lines show the subsequent morphology. $\overline{CV}$ values are provided in the top left of the plots. (For interpretation of the references to colours in this figure legend, the reader is referred to the web version of this article.)

the lack of any clear trend in the seasonal/annual morphological feedback in response to the seasonal signal in the wave conditions. Instead the results suggest that large-scale beach change is dominated by a series of storm events which serve to redistribute material to the lower beach.

The dominant morphological response at PTN and PPT was characterised by rapid transitions towards increased 3D states in the weeks/months following storm wave conditions. These events resulted in the removal of material from the upper beach and accumulation around the low water line. While this response supports previous studies which have shown a flattening of the upper profile (Komar, 1985), here it was observed that the low tide bar/rip features remained present despite the storm waves. As post-storm conditions lead to onshore directed transport during the recovery phase, the weakly 3D shoreline promotes spatially variable deposition which acts to accelerate the development of highly 3D morphology through positive feedback (Castelle et al., 2010). However, continued onshore accretion eventually causes the initial bar/rip features to become increasingly smoothed through in-filling. These periods of 2D transition were observed several times over the survey duration for PTN and PPT occurring over a 3–4 month period. With large storm events often evident in March, the presence of such highly 3D beach states during the summer months is increased, supporting the argument that their formation is primarily a response to calmer accretionary conditions. The results presented support the accretionary development of increased 3D morphology; however, it is also argued this that process is enhanced following storm conditions. The removal of material from the mid/upper beach feeds the subtidal region which supplies material during the accretionary recovery phases. The results deviate from a "seasonal" concept of beach state, and instead imply storm event-driven response, where the "seasonal" climate controls the subsequent morphology. This conclusion is supported, for example, by the distinctive bar/rip morphology which was observed during December 2009 and January 2010 in response to energetic November wave conditions, preceding a gradual straightening of the shoreline (Fig. 12).

By incorporating the $\overline{CV}$ into the conceptual classification scheme proposed by Masselink et al. (2007) the distribution of 3D beach states can be expressed with reference to the relative tidal range (RTR) and the dimensionless fall velocity (Ω) (Fig. 16). The distribution of increased 3D states is centred on the medium energy boundary (H_s = 1.5–2 m), with more planar states present at the more energetic/calmer regions. This supports the field observations where: (1) post storm (energetic) conditions result in increased 3D morphology; and (2) calm conditions lead to infilling and smoothing out of features resulting in reduced 3D. The "optimum" 3D states exist within a central threshold which requires "input" into the system through energetic events to re-distribute the sediment to the lower beach.

For both sites defining a modal state is not clear. The sustained infilling of channels and smoothing of the beach which was observed during the 3–4 month accretionary cycle suggest a shift towards a more planar state. However, despite continued net accretion over the three years of surveys, intermittent storms have led to increased 3D morphology. The balance between storm driven removal and onshore accretion is maintained through episodic events.

The difference in the beach settings is also pronounced and reflects the variability in the morphology observed. PTN has a narrow low tide beach which is backed by steep cliffs and exhibited strong periodicity in bar development and migration with defined channels extending from the cliffs. The central region of the survey area is more likely to be affected by the flows constrained by the narrow upper beach, however, the longshore area displayed strong rhythmicity which suggests that the proximity of the intertidal geology may be important in controlling the nearshore dynamics.

The long-term (years) variability in bar behaviour and orientation has been presented using bar line detection of rectified Argus images at PTN and PPT. Overall, both systems exhibited medium-term stability (weeks–months) of attached nearshore bars. PTN underwent greater variability of bar structure and orientation with highly rhythmic crescentic features dominating the system, whereas PPT was characterised by alongshore rhythmic attached bar behaviour.

The key morphological behaviour during the survey period reflects a strongly storm driven system which is governed by sustained high-energy events. Subsequent morphological response exhibited highly 3D recovery phases before seasonal wave conditions dominated further evolution. Following the removal of material through storm conditions sediment deposition occurred between MLWS and the attached bar. Such processes resulted in more complex bar definition through the increased deposition in this region. These deposits then acted as sources for the post storm onshore transport. This behaviour is comparable to observations in Almar et al. (2010) where crescentic horns developed under storm conditions as material (SPAWs; Shoreward Propagating Accretionary Wave) moved onshore while the bar moved offshore; however, the present study suggests that maximum 3D growth of transverse bars occurs during the recovery phase. Longer term trends in the cross-shore position of the outer break point of the nearshore bars show a strong relationship to the intertidal volume.

Despite the inherent complexities governing the response at each of the sites, the overall behaviour has been well characterised by Fig. 17: (1) offshore transport occurring under sustained large waves, supporting previous field observations (Larson and Kraus, 1994; Lee et al., 1998; Hill et al., 2004; Castelle et al., 2007); and (2) followed by increased 3D morphology not observed in the present literature. The gradual infilling evolution then returns and dominates resulting in the morphology becoming more 2D (Fig. 17). This trend was observed at PTN and PPT several times during the survey period. The rapid post-storm 3D growth is likely to reflect non-uniform wave breaking of small swell-dominated waves which promotes onshore transport. The antecedent morphology and the extent of the storm event determine the post storm low tide

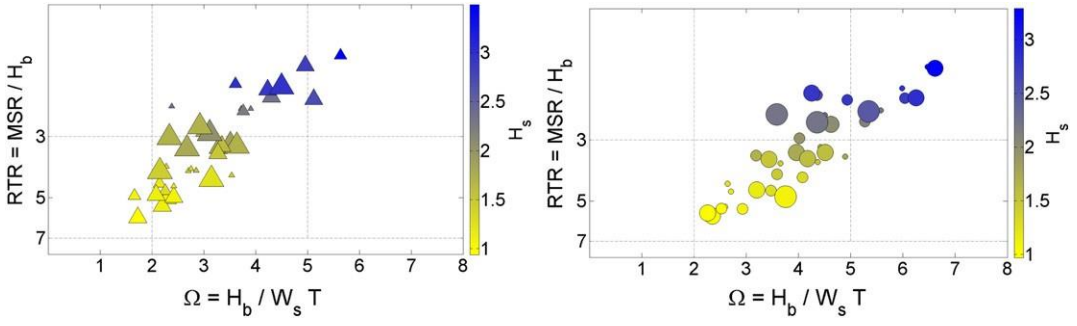

Fig. 16. Conceptual classification of monthly beach states incorporating the relative tidal range (RTR) and dimensionless fall velocity (Ω), based on Masselink et al. (2007). In addition to the trends in wave forcing (yellow shading = calm wave conditions, blue shading = larger waves) the marker size reflects the relative 3D level derived using the $\overline{CV}$ (larger markers indicating more 3D intertidal morphology and smaller markers indicating more planar 2D conditions). (For interpretation of the references to colours in this figure legend, the reader is referred to the web version of this article.)

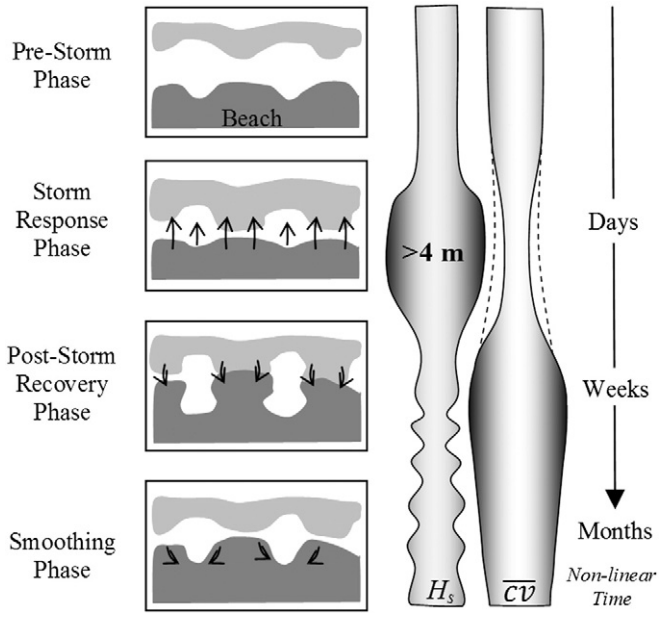

Fig. 17. Schematic diagram of the beach and bar response during and following a storm event. The cycle occurs over a period of two–three months following a sustained large storm, which sees material moved offshore to the subtidal bar (light shading) and returned to the intertidal (dark shading) region as the wave conditions decrease resulting in highly 3D morphology. The relative H_s and $\overline{CV}$ are indicated on the right with larger waves and increased 3D represented by wider columns. Antecedent morphology (planar/3D) dictates the extent of morphological response during the storm event and under post storm recovery phases.

morphology, which in turn dictates subsequent onshore transport and deposition. This behaviour has been observed at these sites however it is likely that similar sandy sites exposed to large waves and macrotidal conditions may well respond in a similar manner.

6. Conclusions

This paper presents and discusses a 3-year morphological dataset collected on two sandy beaches on the high wave-energy and macrotidal coast of north Cornwall which represents the longest record of survey data which has been collected within the UK for these environments. The dataset comprises continuous directional offshore wave data, monthly intertidal beach surveys and daily video data. The three beaches experience a similar tidal regime, but different levels of wave exposure and geological control. The key conclusions are:

1. Despite the macrotidal setting, both beaches are characterised by pronounced inter- and subtidal bar morphology, and can therefore be classified as intermediate beaches. This is confirmed by typical values for the dimensionless fall velocity Ω and relative tide range RTR of 3–5 and 2–4, respectively.
2. All sites experienced progressive intertidal accretion over the monitoring period, but significant monthly morphological variability is present. The envelope of morphological change increases from high to low tide level, and the beach with the greatest overall morphological variability was characterised by the greatest geological control.
3. Despite a seasonal variability in the wave forcing, no corresponding seasonal variation in the intertidal beach volume or inter- and subtidal three-dimensional morphology is apparent.
4. An extended period of energetic wave conditions (N 50 h) is required to generate significant shifts in sediment and changes in the inter- and sub-tidal bar morphology. Any response is dependent on the antecedent morphology and storm events.
5. A conceptual model of morphological change related to very energetic waves was identified, comprising three distinct phases: (1) offshore sediment transport from the inter- to the sub-tidal region and a decrease in three-dimensionality during the energetic wave conditions which generally last up to several days; (2) onshore sediment transport and increased three-dimensionality during the post-storm phase which can take up to a week; and (3) continuing onshore sediment transport, as well as alongshore sediment redistribution, resulting in a smoothing of the three-dimensional morphology during extended (N weeks) calm conditions.
6. In comparison to micro- and meso-tidal beaches exposed to similar wave energy variability, the studied beaches are characterised by long relaxation times. This is attributed to the combination of a large tidal range and a wide and low-gradient intertidal beach profile.

Acknowledgments

This work was undertaken with the support of funding from the South West Regional Development Agency through the Peninsula Research Institute for Marine Renewable Energy (PRIMaRE) and Plymouth University. Fieldwork was supported by Dr Tim Scott and Peter Ganderton. The authors would also like to acknowledge the work of the anonymous reviewers for their comments which helped improve this paper.

References

Almar, R., Castelle, B., Ruessink, B.G., Sénéchal, N., Bonneton, P., Marieu, V., 2010. Two- and three-dimensional double-sandbar system behaviour under intense wave forcing and a meso-macro tidal range. Continental Shelf Research 30 (7), 781–792.

Austin, M.J., Scott, T.S., Russell, P.E., Masselink, G., 2013. Rip current prediction: development, validation and evaluation of an operational tool. Journal of Coastal Research. http://dx.doi.org/10.2112/JCOASTRES-D-12-00093.1.

Battiau-Queney, Y., Billet, J.F., Chaverot, S., Lanoy-Ratel, P., 2003. Recent shoreline mobility and geomorphologic evolution of macrotidal sandy beaches in the north of France. Marine Geology 194 (1–2), 31–45.

Buscombe, D., Scott, T.M., 2008. Coastal geomorphology of North Cornwall: St. Ives to Trevose Head. Internal Report for Wave Hub Impacts on Seabed and Shoreline Processes. University of Plymouth (170 pp.).

Castelle, B., Turner, I.L., Ruessink, B.G., Tomlinson, R.B., 2007. Impact of storms on beach erosion: Broadbeach (Gold Coast, Australia). 9th International Coastal Symposium. Gold Coast. Australia Journal of Coastal Research, pp. 534–539.

Castelle, B., Russeink, B.G., Bonneton, P., Marieu, V., Bruneau, N., Price, T.D., 2010. Coupling mechanisms in double sandbar systems. Part 1: patterns and physical explanation. Earth Surface Processes and Landforms 35 (4), 476–486.

Davidson, M., Huntley, D., Holman, R., George, K., 1997. The evaluation of large-scale (km) intertidal beach morphology on a macrotidal beach using video images. Proceedings Coastal Dynamics 97, 385–394.

Hansen, J.E., Barnard, P.L., 2010. Sub-weekly to interannual variability of a high-energy shoreline. Coastal Engineering 57 (11–12), 959–972.

Hill, H.W., Kelley, J.T., Belknap, D.F., Dickson, S.M., 2004. The effects of storms and storm-generated currents on sand beaches in Southern Maine, USA. Marine Geology 210 (1–4), 149–168.

Holland, K.T., Holman, R.A., Lippmann, T.C., Stanley, J., Plant, N., 1997. Practical use of video imagery in nearshore oceanographic field studies. IEEE Journal of Oceanic Engineering 22 (1), 81–92.

Holman, R.A., Stanley, J., 2007. The history and technical capabilities of Argus. Coastal Engineering 54 (6–7), 477–491.

Jago, C.F., Hardisty, J., 1984. Sedimentology and morphodynamics of a macrotidal beach, Pendine Sands, SW Wales. Marine Geology 60 (1–4), 123–154.

Kingston, K.S., Ruessink, B.G., van Enckevort, I.M.J., Davidson, M.A., 2000. Artificial neural network correction of remotely sensed sandbar location. Marine Geology 169 (1–2), 137–160.

Komar, P.D.B.C., 1985. Analysis of grain-size measurements by sieving and settling-tube techniques J Sediment Petrol V54(N2), June 1984, pp. P603–614. International Journal of Rock Mechanics and Mining Science and Geomechanics Abstracts 22 (3), A80–A81.

Larson, M., Kraus, N.C., 1994. Temporal and spatial scales of beach profile change, Duck, North Carolina. Marine Geology 117 (1–4), 75–94.

Lee, G.-h, Nicholls, R.J., Birkemeier, W.A., 1998. Storm-driven variability of the beach-nearshore profile at Duck, North Carolina, USA, 1981–1991. Marine Geology 148 (3–4), 163–177.

Lippmann, T.C., Holman, R.A., 1990. The spatial and temporal variability of sand bar morphology. Journal of Geophysical Research 95 (C7), 11575–11590.

Masselink, G., Auger, N., Russell, P., O'Hare, T., 2007. Short-term morphological change and sediment dynamics in the intertidal zone of a macrotidal beach. Sedimentology 54 (1), 39–53.

Merefield, J.R., 1984. Modern cool-water beach sands of Southwest England. Journal of Sedimentary Research 54 (2), 413–424.

Plant, N. G., Holland, K., T. & Puleo, J. A. (2008) 'Application of quadratic loess filters to bathymetric interpolation', Unpublished. Naval Research Lab, pp. 37.

Poate, T.G., 2012, Morphological response of high-energy macrotidal beaches. Unpublished thesis, Plymouth University, 260 pp.

Poate, T.G., Kingston, K.S., Masselink, G., Russell, P., 2009. Response of high-energy, macrotidal beaches to seasonal changes in wave conditions: examples from North Cornwall, UK. Journal of Coastal Research SI 56, 747–751.

Ranasinghe, R., Symonds, G., Black, K., Holman, R., 2004. Morphodynamics of intermediate beaches: a video imaging and numerical modelling study. Coastal Engineering 51 (7), 629–655.

Reichmüth, B., Anthony, E.J., 2007. Tidal influence on the intertidal bar morphology of two contrasting macrotidal beaches. Geomorphology 90 (1–2), 101–114.

Ruggiero, P., Kaminsky, G.M., Gelfenbaum, G., Voigt, B., 2005. Seasonal to interannual morphodynamics along a high-energy dissipative littoral cell. Journal of Coastal Research 21 (3), 553–578.

Schlax, M.G., Chelton, D.B., 1992. Frequency domain diagnostics for linear smoothers. Journal of the American Statistical Association 87 (420), 1070–1081.

Scott, T.M., Russell, P.E., Masselink, G., Wooler, A., Short, A., 2007. Beach rescue statistics and their relation to nearshore morphology and hazards: a case study for south-west England. 9th International Coastal Symposium Gold Coast, Australia 16–20 April. CERF.

Scott, T., Masselink, G., Russell, P.E., 2011. Morphodynamic characteristics and classification of beaches in England and Wales. Marine Geology 286, 1–20. http://dx.doi.org/10.1016/j.margeo.2011.04.004.

Short, A.D., 1996. The role of wave height, period, slope, tide range and embaymentisation in beach classifications: a review. Revista Chilena de Historia Natural 69, 589–604.

Smit, M.W.J., Reniers, A.J.H.M., Symonds, G., Ruessink, B.G., 2008. Morphodynamic modelling of up-state and down-state transitions at Palm beach, NSW, Australia. In: Smith, J.M. (Ed.), Coastal Engineering. Hamburg World Scientific, pp. 2437–2445.

van Enckevort, I.M.J., Ruessink, B.G., 2001. Effects of hydrodynamics and bathymetry on video estimates of nearshore sandbar position. Journal of Geophysical Research 106, 16969–16979.

Wright, L.D., Nielsen, P., Short, A.D., Green, M.O., 1982. Morphodynamics of a macrotidal each. Marine Geology 50 (1–2), 97–127.

Wright, L.D., Short, A.D., Green, M.O., 1985. Short-term changes in the morphodynamic states of beaches and surf zones: an empirical predictive model. Marine Geology 62 (3–4), 339–364.